IEEE Robotics and Automation Letters (RA-L) paper, presented at ICRA 2026, Vienna, Austria. Cite as RA-L paper.

A 3 Degrees-of-Freedom Lightweight Flexible Twisted String Actuators (TSAs)-Based Exoskeleton for Wrist Rehabilitation

Mihai Dragusanu, *Member, IEEE*, Nicolas Guinet, Bhivraj Suthar, *Member, IEEE*, Tommaso Lisini Baldi, *Member, IEEE*, Domenico Prattichizzo, *Fellow, IEEE*, and Monica Malvezzi, *Member, IEEE*

***Abstract*—This letter introduces a lightweight, three-degrees-of-freedom exoskeleton for wrist rehabilitation powered by Twisted String Actuators (TSAs), specifically designed to support flexion/extension, radial/ulnar deviation, and pronation/supination movements. Leveraging the high power-to-weight ratio of TSA actuation system, the exoskeleton ensures effective, comfortable, and personalized rehabilitation exercises. The device comprises five TSAs arranged in a tendon-driven configuration, enabling precise control and adaptability to various user anatomies. The experimental evaluations was conducted on a prototype demonstrating the device's ability to accurately replicate wrist movements guided by a physiotherapist, achieving low tracking errors (RMSE $\leq$ 1°). The exoskeleton effectively achieves the desired wrist range of motion—115° for flexion/extension, 70° for radial/ulnar deviation, and 150° for pronation/supination—with torque capabilities suitable for rehabilitation purposes (0.35 Nm for flexion/extension and radial/ulnar deviation, and 0.06 Nm for pronation/supination).**

***Index Terms*—Wearable robotics, rehabilitation robotics, soft robot materials and design, prosthetics and exoskeletons, tendon/wire mechanism.**

I. Introduction

WRIST injuries and disorders, ranging from carpal tunnel syndrome to fractures and tendonitis, have become increasingly common in today's fast-paced, tech-driven world. For individuals affected by these conditions, effective rehabilitation is vital to restore mobility and function. Traditional rehabilitation methods require prolonged commitment from both patients and therapists. The sustained effort and scheduling constraints can slow progress and make the experience burdensome, both physically and mentally, for patients, a This challenge has driven the evolution of robot-based rehabilitation strategies, which represent a promising alternative to improve the efficiency and outcomes of rehabilitation process by reducing the need for constant human supervision [1], [2], [3], [4].

In the quest for developing more advanced robotic systems for rehabilitation, various actuator technologies have been explored. Cable-driven actuators have been among the earliest and most widely adopted due to their simple design and high force output. These systems can allow slack in the cable, which, in some cases, results in zero added impedance, which makes them favorable for applications requiring minimal resistance when not in use [2], [5]. However, cable-driven actuators often require additional components like pulleys and gears to generate necessary torques, leading to increased inertia, which can limit their usefulness, especially in wearable devices.

Twisted String Actuators (TSA) represent an interesting solution in cable-driven mechanisms. In a TSA, an electric motor twists a string, generating a linear pulling motion without the need of transmission mechanisms, reducing weight and encumbrance, leading to a more compact and efficient actuation system [6]. Such properties make TSAs especially suitable for wearable robotics, where portability and precision are critical [7], [8]. Compared to traditional pneumatic or hydraulic actuators, TSAs are considerably lighter, more energy-efficient, and capable of generating precise movements [9], [10]. TSAs have been applied in numerous robotic systems, showcasing their versatility. The DEXMART anthropomorphic robotic hand utilizes 24 independent TSAs to achieve dexterity and fine control [11]. The Auxilio exoskeleton, designed for elbow and shoulder support, harnesses TSA technology to provide a lightweight solution for upper-limb assistance [12]. The ExoTen-Glove, a TSA-powered haptic interface for virtual reality, highlights the potential of TSAs in applications requiring both precision and minimal bulk [13].

The human wrist is a particularly complex joint, with multiple DOFs that demand precise control to achieve successful rehabilitation outcomes. TSAs are flexible and adaptable solutions for designing exoskeletons capable of accommodating the movements of the wrist [14], [15]. TSA adaptability enables

Received 28 December 2024; accepted 18 April 2025. Date of publication 8 May 2025; date of current version 20 May 2025. This article was recommended for publication by Associate Editor V. Vashista and Editor P. Valdastri upon evaluation of the reviewers' comments. This work was supported in part by the European Union by the Next Generation EU Project ECS17 THE - Tuscany Health Ecosystem (PNRR MUR M4 C2 Inv. 1.5, CUP B63C22000680007, Spoke 9: Robotics and Automation for Health). *(Corresponding author: Mihai Dragusanu.)*

This work involved human subjects or animals in its research. Approval of all ethical and experimental procedures and protocols was granted by Ethical Committee of the University of Siena "CAREUS" for Research in the Human and Social Sciences, and performed in line with the declaration of Helsinki.

Mihai Dragusanu, Nicolas Guinet, Tommaso Lisini Baldi, and Monica Malvezzi are with the Department of Information Engineering and Mathematics, University of Siena, 53100 Siena, Italy (e-mail: mihai.dragusanu2@gmail.com; n.guinet@student.unisi.it; tommaso.lisini@unisi.it; monica.malvezzi@unisi.it).

Bhivraj Suthar is with the School of Artificial Intelligence and Data Science, Indian Institute of Technology Jodhpur (IITJ), Jodhpur 342030, India (e-mail: bhivraj@iitj.ac.in).

Domenico Prattichizzo is with the Department of Information Engineering and Mathematics, University of Siena, 53100 Siena, Italy, and also with the Humanoids & Human Centered Mechatronics Research Line, Istituto Italiano di Tecnologia, 16163 Genoa, Italy (e-mail: dprattichizzo@unisi.it).

This article has supplementary downloadable material available at https://doi.org/10.1109/LRA.2025.3568305, provided by the authors.

Digital Object Identifier 10.1109/LRA.2025.3568305

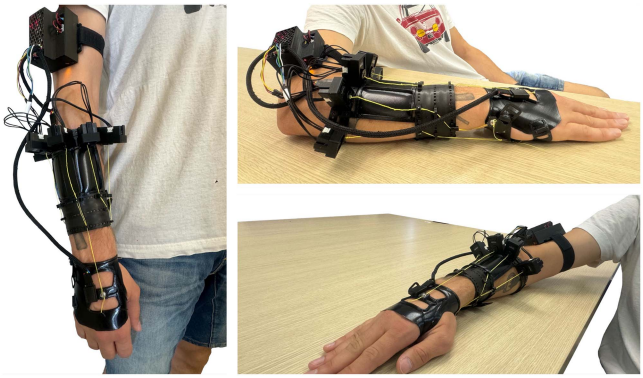

Fig. 1. The TSA-based tendon-driven wrist exoskeleton prototype worn by a user.

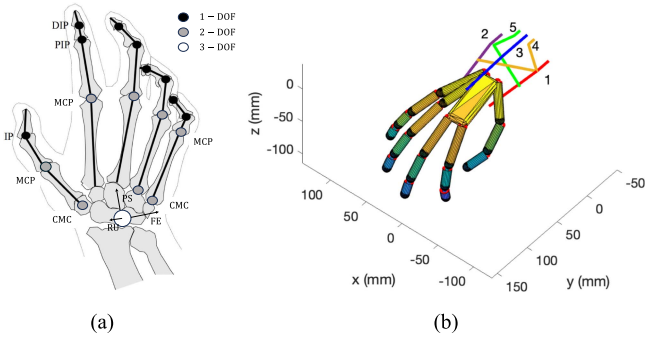

(a) (b)

Fig. 2. Hand/wrist biomechanical schemes. (a) The 28-DOFs biomechanical hand/wrist model, consisting of a 25-DOFs hand model, and 3 DOFs for the wrist. (b) Graphical representation of the hand Syngrasp model integrated with the 5 actuated tendons for wrist motion support [22]. .

the exoskeleton to provide customized support and resistance, tailored to the specific needs of rehabilitation. The ability of TSAs to precisely adjust to these movements can enhance the effectiveness of rehabilitation, ensuring that the device can respond dynamically to varying forces and movements during rehabilitation [16], [17]. Recent studies [6], [16], [18] present TSA-powered exoskeleton devices, highlighting their suitability for wrist and hand rehabilitation.

This letter presents the design, implementation, and evaluation of a TSA-based exoskeleton designed for wrist rehabilitation (Fig. 1). The exoskeleton is lightweight, flexible, and can be effective in assisting patients in their rehabilitation journey [19], [20]. Its compactness makes it less intrusive and more comfortable, while the high power-to-weight ratio ensures effective assistance during rehabilitation exercises. This device aims to enhance recovery outcomes for individuals suffering from wrist-related injuries and disorders, accelerating their return to normalcy. The device stands out for its modular, ergonomic, and customizable design, adapting to the user's dimensions through a parametric approach. Its tendon-driven system allows easy tendon routing adjustments via specialized components, optimizing movement execution. Additionally, an integrated fastening system enables tendon length adjustments, while a tendon release mechanism ensures safety in case of emergencies or motor malfunctions. The system also guarantees maximum freedom of wrist movement, minimizing the device's encumbrance. To enhance position control, a closed-loop tracking system has been integrated, and a graphical user interface has been developed. This enables the execution of both predefined and customized exercises. The system can record and store movement profiles performed by a specialist, allowing the user to reproduce them later. In the current implementation, the device operates in passive mode, moving the user's wrist without requiring any effort from the patient.

The letter is organized as follows. Section II introduces the main design requirements, Section III presents a kinematic model and analysis of the hand/wrist system wearing the tendon-driven exoskeleton, Section IV introduces the design and prototype of the exoskeleton, Section V presents some evaluation tests realized with the prototype worn by a user, Sections VI and VII summarize the main exoskeleton characteristics and present some concluding remarks.

II. Design Requirements

The system was developed for a patient with limited active hand and wrist control, reduced residual strength, low muscle tone, and minimal spasticity. Such conditions often result from neurological conditions such as stroke or Limb-Girdle Muscular Dystrophy. In the chronic phase of such diseases, even small, repetitive wrist movements reflect the principle that frequent, task-oriented practice helps maintain neuromuscular function and joint range of motion over time. For instance, Lang et al. [21] observed in stroke rehabilitation settings that the number of small, repeated movements is correlated with better functional outcomes. Although the device is designed for a specific user, the modularity and flexibility of structural parts make it adaptable to other users with different needs.

A. Hand and Wrist Biomechanics

Although the device proposed in this letter focuses on wrist actuation, we consider a comprehensive hand-wrist biomechanical model. This is because the anchor points are connected to the palm and the device is designed as a modular component that can be integrated with the glove presented in [6]. The kinematic analysis is applied to a 28-DOFs biomechanical model of the hand-wrist implemented with Syngrasp Toolbox [22]. Its scheme is reported in Fig. 2(a). The wrist is modeled as a 3-DOFs spherical joint, while for the hand, we considered the model from [23]. We chose this model due to its completeness in hand motion representation and easy adaptability to different hand sizes and characteristics [24], since all the link dimensions can be varied by changing two parameters, i.e. hand length and hand width. The wrist motion can be represented as a 3-DOFs spherical joint, including flexion/extension (FE), radial/ulnar (RU) deviation, and pronation/supination (PS). The thumb is modeled as a 5-DOF system: 2 DOFs (adduction/abduction and extension/flexion) for the carpometacarpal (CMC) joint, 2 DOFs (extension/flexion and adduction/abduction)for the metacarpophalangeal (MCP) joint, and 1 DOF (extension/flexion) for the interphalangeal (IP) joint. The index and middle fingers are modeled as two 4-DOFs systems: 2-DOFs (extension/flexion, adduction/abduction) for the MPC joints, 1-DOF (extension/flexion) for the proximal-interphalangeal (PIP) and distal-interphalangeal (DIP) joints. The ring and the little fingers are modeled as two 6-DOFs systems: two 2-DOFs for the CMC joints, to provide the palm arc motion, 2-DOFs for the MPC joints, and 1-DOF for the PIP and DIP joints.

IEEE Robotics and Automation Letters (RA-L) paper, presented at ICRA 2026, Vienna, Austria. Cite as RA-L paper.

TABLE I
ROM AND TORQUE REQUIREMENTS FOR WRIST ACTUATION

Motion	ROM (degrees)	Torque (Nm)
Flexion/extension	115	0.35
Radio/Ulnar deviation	70	0.35
Prono/supination	150	0.06

B. Range of Motion (ROM) and Torque Requirements

We referred to studies available in the literature: a review of the functional kinematics of the healthy and injured wrist is presented by Rainbow et al. [25], while Park et al. present results on impedance properties of the wrist obtained through in-vivo measurements [26]. As a reference for wrist and upper limb kinematic requirements, we considered the values proposed by Perry and Burns [27], which experimentally analyzed upper limb workspace and ROM by realizing a database compiled from 19 arm activities of daily living. These requirements were considered by Wu et al. [28] in the design of a 5-DOF elbow and wrist exoskeleton. The joint ROM and torque limits used in this letter are summarized in Table I.

III. TENDON ACTUATED SYSTEM ANALYSIS

A preliminary model of a tendon-driven actuated glove was introduced in [6] for a specific implementation for hand fingers. In this letter, we systematically extend and generalize the procedure,which can be applied to both hand fingers and wrist actuation.

Let us indicate with $\mathbf{q} \in \Re^{n_q}$ the joint vector, i.e. a vector containing the joint angular configurations. For the hand/wrist system previously introduced, $n_q = 28$, specifically, indices ranging from 1 to 25 refer to hand joints, q_{26} represents pronation/supination movement, q_{27} represents radial/ulnar deviation, and q_{28} represent wrist flexion/extension.

A tendon anchor point $A_{j,f,l,i}$ is defined by specifying: (1) the tendon index j: an integer positive numerical tag for tendon identification, j varies from 1 to n_t, number of tendons; (2) the finger index f: an integer positive numerical tag for forearm/palm/finger identification, varying from -1 (forearm) to $n_f = 5$ (little finger); (3) the link index l, an integer numerical tag for link identification, within the finger, varying from 0 to the number of links of the specific finger $n_{l,f}$ (the palm and the forearm have one link only, indicated with 0); (4) an integer positive index i for indicating the order of the anchor in the tendon routing, starting from 1, the point where the tendon end is fixed on the finger or the palm, and increasing towards the actuator, up to $n_{a,j}$ (i.e., $n_{a,j}$ represents the number of anchor points of tendon j); (5) and the coordinates $\mathbf{r}_a^{f,l} = [x_a^{f,l}, y_a^{f,l}, z_a^{f,l}]^{\mathrm{T}}$ of the anchor point, expressed in the local link reference frame $\mathcal{S}_{f,l}$, on the l-th link of the f-th finger, where the anchor point is connected.

Standard forward kinematics relationships allow the evaluation of anchor points' position during hand and wrist motion. In particular, for a given configuration represented by joints $\mathbf{q}$, the coordinates of the generic anchor point in the base (forearm) reference frame can be defined as:

$$\tilde{\mathbf{r}}_{i,j} = \mathbf{T}_0^{f,l} \tilde{\mathbf{r}}_{i,j}^{f,l}, \tag{1}$$

where $\mathbf{T}_0^{f,l} \in \Re^{4\times4}$ is the homogeneous transformation matrix between the base reference frame and the link reference frame, depending on the hand's configuration, that can be evaluated for example using Denavit-Hartenberg parameters, and $\tilde{\mathbf{r}}_a$ and $\tilde{\mathbf{r}}_i^{f,l}$ are the homogeneous representations of $\mathbf{r}_{i,j}$ and $\mathbf{r}_{i,j}^{f,l}$, respectively (i.e. $\tilde{\mathbf{r}}_a = [\mathbf{r}_a^{\mathrm{T}}, 1]^{\mathrm{T}}$). Given the positions of the anchor points of the j-th tendon, defined in the base reference frame, the corresponding tendon length l_j can be evaluated as:

$$l_j = \sum_{i=1}^{n_{a,j}-1} ||\mathbf{r}_{i+1,j} - \mathbf{r}_{i,j}||, \tag{2}$$

where $n_{a,j}$ is the number of anchor points in the j-th tendon. Tendon lengths are collected in the vector $\mathbf{l} = [l_1, \ldots, l_{nt}]^{\mathrm{T}} \in \Re^{n_t}$. The displacement that has to be applied by the actuator is then evaluated as: $s_j = l_{j,0} - l_j$, where $l_{j,0}$ is tendon length in hand reference configuration. Let us further collect the positions of all the anchor points in a vector $\mathbf{r}_a = [\mathbf{r}_{1,1}^{\mathrm{T}}, \ldots, \mathbf{r}_{n_t,n_{a,nt}}^{\mathrm{T}}]^{\mathrm{T}} \in \Re^{3n_a}$, where $n_a = \sum_{j=1}^{n_t} n_{a,j}$.

Standard differential kinematics relationships can be straightforwardly used to define the anchor point Jacobian matrix $\mathbf{J}_a \in \Re^{3na\times n_q}$ relating anchor point velocities $\mathbf{v}_a = [\mathbf{v}_{a,1,1}^{\mathrm{T}}, \ldots, \mathbf{v}_{a,n_t,n_{a,nt}}^{\mathrm{T}}]^{\mathrm{T}} \in \Re^{3na}$, where $\mathbf{v}_{a,i} = \frac{d\mathbf{r}_i}{dt}$ is the velocity of the i-th anchor point, to joint angular velocities $\dot{\mathbf{q}}$, namely $\mathbf{v}_a = \mathbf{J}_a\dot{\mathbf{q}}$. Let us consider a generic pair of adjacent anchor points $A_{i,j}$, $A_{i+1,j}$ on the generic tendon, j. The previously introduced equation allows us to evaluate their velocities $\mathbf{v}_{a,i,j}$ and $\mathbf{v}_{a,i+1,j}$ for a given hand configuration and velocity. The time derivative of tendon length between such points is defined by:

$$\dot{l}_{(i,i+1),j} = (\mathbf{v}_{a,i,j} - \mathbf{v}_{a,i+1,j}) \cdot \mathbf{u}_{i-i+1,j}, \tag{3}$$

where $\mathbf{u}_{i-i+1,j}$ is the unit vector identifying the direction between $A_{i,j}$ and $A_{i+1,j}$ points. The overall tendon velocity is defined as:

$$\dot{l}_j = \sum_{i_1}^{n_{a,j}-1} \dot{l}_{(i,i+1),j} = \sum_{i_1}^{n_{a,j}-1} \mathbf{u}_{i-i+1,j}^{\mathrm{T}}(\mathbf{v}_{a,i,j} - \mathbf{v}_{a,i+1,j}), \tag{4}$$

that can be rewritten as $\dot{l}_j = \mathbf{J}_{t,j}\mathbf{v}_{a,j}$, where: $\mathbf{J}_{t,j} = [\mathbf{u}_{1,j}, -\mathbf{u}_{1,j} + \mathbf{u}_{2,j}, \ldots, -\mathbf{u}_{n_{a,j},j}]$. By analyzing anchor point velocities it is possible to define a relationship between tendon velocities $\dot{\mathbf{l}} = [\dot{l}_1, \ldots, \dot{l}_{n_a}]^{\mathrm{T}}$ and anchor point velocities $\mathbf{v}_a$, namely $\dot{\mathbf{l}} = \mathbf{J}_t\mathbf{v}_a$. Therefore, a relationship between tendon velocities and hand joint angular velocity can be established as $\dot{\mathbf{l}} = \mathbf{J}\dot{\mathbf{q}}$, where $\mathbf{J} = \mathbf{J}_t\mathbf{J}_a \in \Re^{n_t\times n_q}$ is the exoskeleton Jacobian. It is possible to define a relationship between hand/wrist joint torques $\boldsymbol{\tau} \in \Re^{n_q}$ and tendon forces $\mathbf{f} \in \Re^{n_t}$, i.e., $\boldsymbol{\tau} = \mathbf{J}^{\mathrm{T}}\mathbf{f}$. To implement a force control on the device, such relationship has to be inverted, i.e. a set of tendon forces $\mathbf{f}$ have to be defined to obtain a certain torque $\boldsymbol{\tau}$. If we consider wrist actuation only, we can assume for the sake of conciseness $n_q = 3$. The device that will be presented in the following section for wrist actuation is actuated by $n_t = 5$ actuators, so for this sub-problem, the transpose of the Jacobian matrix $\mathbf{J}^{\mathrm{T}}$ dimensions are 3×5. If the matrix is full-rank, the linear system in eq. (III) has infinite solutions, that can be represented as:

$$\mathbf{f} = (\mathbf{J}^{\mathrm{T}})^{+}\boldsymbol{\tau} + \mathbf{N}_{Jt}\boldsymbol{\xi} \tag{5}$$

where $\mathbf{N}_{Jt}$ is a basis of $\mathbf{J}^{\mathrm{T}}$ nullspace and $\boldsymbol{\xi}$ is an arbitrary vector. Force vectors defined by $\mathbf{f}_i = \mathbf{N}_{Jt}\boldsymbol{\xi}$ represent the set of

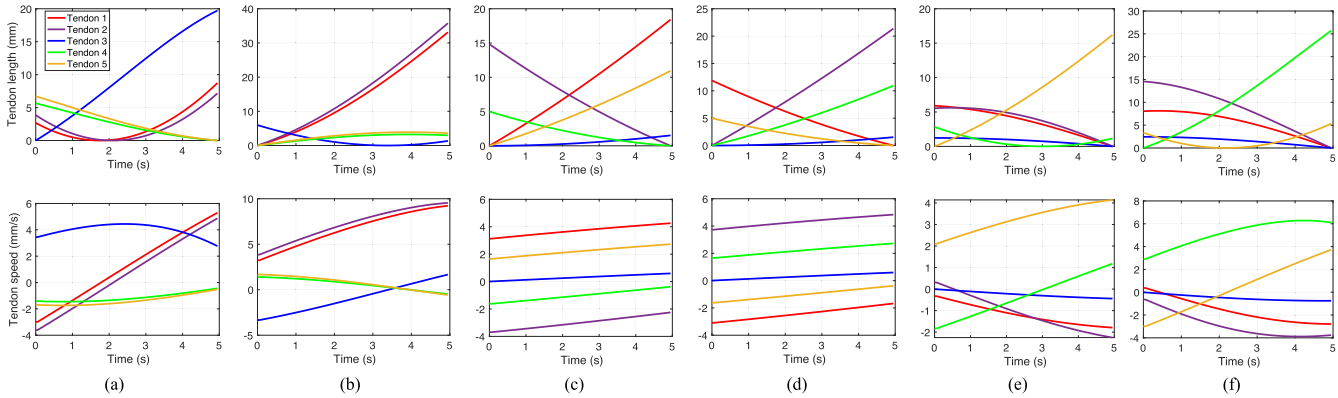

Fig. 3. Simulation results: tendon lengths and speeds. a) Wrist extension, $q_{28} = 90°$. b) Wrist flexion $q_{28} = -90°$. c) Ulnar deviation, $q_{27} = 35°$. d) Radial deviation, $q_{28} = -35°$. e) Pronation, $q_{26} = -30°$, f) Supination, $q_{26} = 90°$.

tendon forces that do not apply torques to hand and wrist joint. Such forces can be exploited in device control for example to guarantee that tendons are tight during the whole exercise.

In the device proposed in this letter, tendons are actuated by TSA. Therefore, the analysis should be complemented by including the actuator transmission, i.e., the relationship between tendon length variation s_j and motor rotation θ_j. This aspect is important, due to the peculiar non-linear behavior of this type of actuator, and has been comprehensively investigated in previous studies, e.g. [9], [10].

A. Numerical Simulations

The kinematic model of the hand/wrist and tendons was implemented in Syngrasp [22] (Fig. 2(b)). Simulations of rehabilitation exercises, based on the kinematic requirements summarized in Table I, were carried out to determine the tendon strokes and velocities necessary for specific movements. This information is important for defining the TSAs' characteristics in the device development phases.

In the proposed configuration, five tendons were used to actuate wrist movements. Two tendons, labeled 1 and 2 in Fig. 2(b), connect the forearm to two points on the palm below the hand's coronal plane. When these tendons are pulled synchronously, they enable wrist flexion, while opposite strokes actuate radial and ulnar deviation. Tendon 3 connects the forearm to the back of the hand and actuates wrist extension. The anchor points for this tendon are located approximately on the sagittal plane of the hand. Tendons 4 and 5 connect the forearm to two points on the palm near the carpus. Their crossed routing allows the actuation of pronation and supination movements. The anchor point positions on the hand and the forearm (i.e. $\mathbf{r}_a^{f,l}$) were chosen to guarantee the correct wrist motion transmission when the tendons are actuated. On the forearm, the anchor points are near the wrist, at a distance that allows for incorporating them on a bracelet.

Specific MATLAB functions were developed and integrated in Syngrasp. The simulation results for wrist extension/flexion, radial-ulnar deviation, and pronation-supination movements are reported in Fig. 3. Each movement was performed over a duration of 5 s, with amplitudes defined based on the kinematic constraints in Table I. The results indicate that for the specific user and device parameters, wrist extension can be achieved by pulling tendon 3 with a stroke of $l_3 = 20$ mm, while wrist flexion requires pulling tendons 1 and 2 with strokes of $l_1 = 30$ mm and $l_2 = 32$ mm. Radial and ulnar deviations are obtained by opposite activation of tendons 1 and 2, while pronation and supination movements are achieved by pulling tendons 4 and 5.

TSAs and tendons generate force only by pulling, resulting in positive stroke values in Fig. 3. During exercises, some tendons are pulled while others are released, requiring appropriate pre-stretch values. For example, in wrist extension Fig. 3, tendon 3 is pulled, tendons 4 and 5 are released, and tendons 1 and 2 are initially released and then pulled. Proper pre-stretching, achieved through TSA pre-twists, ensures correct exercise execution.

IV. Implementation

A. Prototype

The wrist exoskeleton consists of two main components: the hand and the forearm supports. The hand support includes a glove with tendon-fixing anchor points, while the forearm support consists of two bands and a part that interconnects them and contains the support for the actuation unit and the tunnel anchor points used to route tendons along the forearm. The prototype worn by a user is shown in Fig. 1.

The actuation system is based on the scheme reported in Fig. 2(b). Each tendon consists of a pair of strings routed along the forearm and firmly fixed, on one side to the motor shaft and on the other to the fixing points on the hand. The strings (polyethylene Dyneema fiber, Japan), have a diameter of 0.4 mm and can withstand tensile forces up to 450 N. The motors (Dynamixel XL330-M077-T, Robotis, South Korea) apply the TSA principle to induce tendon contraction. The motors are lightweight, compact, and require low voltage, have a stall torque of 0.228 Nm and angular speed of 456 rev/min, making them ideal for TSA applications [29]. Due to the TSA principle, the motors require lower current compared to traditional cable-pulling actuators, since the pulling force is generated by cable twisting.

The system is controlled by an OpenCM9.04 board featuring a 32-bit Arm Cortex-M3 microcontroller, which processes data from two Inertial Measurement Units (IMUs) employed for exoskeleton tracking. Power is supplied by two 3.7 V Li-Po batteries, regulated to provide 6 V for maximum motor speed. Device movements are monitored via a graphical user interface (GUI) and can be controlled through USB or Bluetooth communication, using the RN-42 Bluetooth module (Roving Networks Inc., US). All electronic components are housed in a box, with

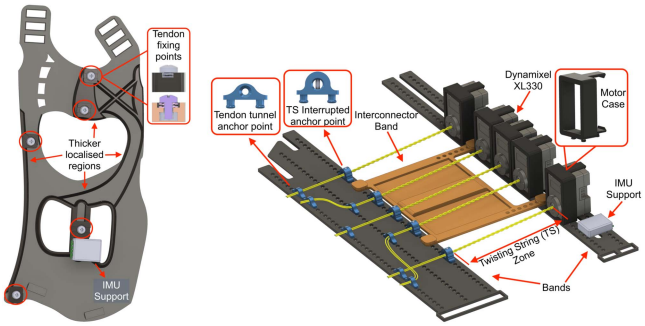

Fig. 4. The 3D-CAD flexible wrist exoskeleton. a) Support for the hand. b) Support for the forearm.

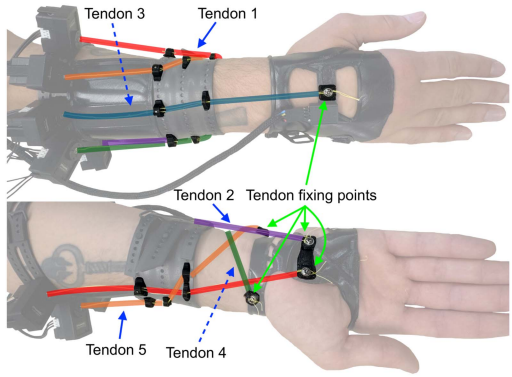

Fig. 5. Tendon routing for wrist actuation. Tendons 1,2, and 3 actuate flexion/extension and abduction/adduction, while tendons 4 and 5 actuate pronation/supination.

an external button for powering the device on/off, ensuring user safety.

1) Hand Support: The hand support is made of Thermoplastic Polyurethane (TPU) to ensure comfort and proper adherence to the user's hand. Its CAD model is reported in Fig. 4(a). The glove design accommodates different hand sizes, covering the wrist to the first knuckles, with sections tailored for the thumb and the bottom of the hand, allowing full finger mobility while wearing the device. Tendon fixing points, highlighted with red circles in Fig. 4(b), are made of PLA and include an M3 nut embedded during the 3D printing phase and an M3 bolt for tendons manual pre-stretching. Serrated washers prevent tendon slippage under high force. The support thickness is variable, according to specific structural analyses (not reported in this letter for the sake of space) to guarantee a proper trade-off between support flexibility for user's comfort and structural deformation when the tendons are activated.

2) Forearm Support: The forearm support, made of TPU material, consists of two adjustable bands and an interconnecting part, as shown in Fig. 4(b). The bands secure the exoskeleton to the forearm, house the actuation unit, and guide the tendons through tunnel anchor points. Adjustable band holes accommodate various forearm sizes and allow precise motor positioning to align with tendon paths. According to user's needs, each motor can be positioned along the strap using motor case pins. The interconnecting part implements the TSA. Each TSA consists of an actuator and two strings connected to the motor shaft. The twisting string (TS) zone is fundamental for TSA implementation. It is the zone between the motor shafts and specific anchor points, as shown in Fig. 4(b). These anchor points consist of a PLA-made flat base with two pins and half-cylindrical extrusions that guide the tendon routing.

The string twisting zone is fundamental for TSA implementation, and is delimited by specific anchor points visible in Fig. 4(b) consisting of a PLA-made flat base with two pins and half-cylindrical extrusions for tendon routings. These components are adjustable along the first forearm band to align with tendon paths. The interconnecting part has thicker sections to prevent slippage and ensure user safety.

3) Tendon Routing: The tendon routing system follows the scheme discussed in Section III. To perform wrist motions, the tendon fixing points are placed on the glove, with the following configuration: one on the hand back center, two on the palm (one on left and one on the right side), one below the thumb finger, and one below the little finger (Fig. 5). The first three tendons are routed along the neutral axis, i.e. the axis formed by the hand and the forearm when aligned. Actuating the tendon 3 and releasing tension from tendon 1 and tendon 2, extends the wrist, while synchronously activating the tendon 1 and tendon 2 and releasing tendon 3 flexes the wrist. When actuating asynchronously the tendons 1 and 2, attached to hand palm, while keeping fixed tendon 3, the abduction/adduction movements are obtained. The other two tendons activate the pronation/supination movements. However, the force required for these rotational motions cannot be applied directly along the neutral axis of the forearm. To achieve effective forearm rotation, the tendons are routed below the forearm in a crossed pattern (Fig. 5). To guide the tendons from the motors to the glove, according to this crossed path, specific tunnels are used that can be easily moved around the forearm through multiple holes present on the bracelet. These elements, highlighted in Fig. 4(b), are 3D-printed in PLA, and consist of a flat base with two pins. Fig. 5 shows the complete tendons routing system.

B. Tracking and Control: The system tracks hand and wrist motions using two MinIMU-9 v5 (Pololu Corporation, USA) sensors, each integrating an accelerometer, gyroscope, and magnetometer. One sensor is placed on the forearm motor bands and the other on the hand's back. Using the algorithm from [4], it determines hand orientation relative to the forearm, enabling motion recording, exercise monitoring, and range of motion analysis. The exoskeleton is controlled via a GUI that communicates with the device through its embedded Bluetooth module. The OpenCM 9.04 processes motor control and IMU data, sending feedback to the GUI.

As observed in Section III-A, all the tendons must be pretensioned before using the device, so each TSA must be pretwisted. The pre-tension of the tendons depends on the user's anthropometric dimensions. The pre-tension can be evaluated based on the positions of the fixing points, with the mathematical model described in Section III-A, and the calibration procedure included in the GUI. The wrist exoskeleton is controlled in position, based on IMU data. The stiffness can be regulated by selecting the proportional gain in a predefined range. The input for controlling the prototype is a reference wrist movement $\mathbf{q}_{des} \in \Re^3$, that can be chosen by the user among a library of pre-defined time-dependent profiles or exercise previously recorded by the tracking system. Then the position error configuration $\tilde{\mathbf{q}} = \mathbf{q}_{des} - \mathbf{q}$ is transformed into references for the TSAs $\boldsymbol{\theta}_{des} \in \Re^5$. The actual wrist position $\mathbf{q}$, measured by the

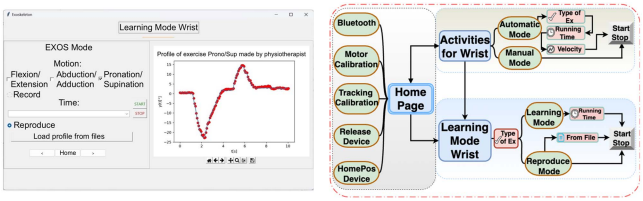

(a) (b)

Fig. 6. a) GUI display during a Reproduce layout in Learning Mode for wrist pronation/supination exercise. b) GUI flow chart for wrist exercises.

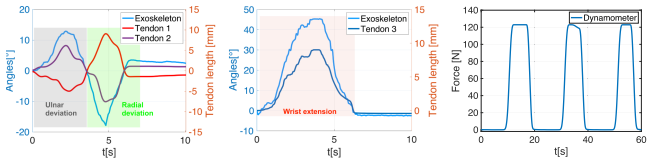

(a) (b) (c)

Fig. 7. Kinematic and force evaluation. (a,b) Wrist rotation angles and tendons' length variations, two sample trials. a) Ulnar deviation. b) Wrist extension c) Measure of TSA force.

tracking system, is also displayed on the GUI and logged during the exercise execution.

C. Graphical User Interface: A cross-platform Python GUI was developed for intuitive control of the wrist exoskeleton. It features three pages: one for calibration and system settings, and two for specific functions. Default parameters ensure safe operation, preventing activation if incorrectly set. The GUI supports Bluetooth and USB connections, allowing real-time storage and playback of wrist motions for rehabilitation and training. Additionally, specialists can monitor and adjust the user's rehabilitation process online using the stored data. A screenshot of the application is shown in Fig. 6(a) while a flowchart reporting all the GUI elements is reported in Fig. 6(b). In the following, the GUI main pages are briefly detailed.

Home Page: provides general functions for connecting or disconnecting the exoskeleton via Bluetooth, calibrating the device, and accessing other pages. After connection, the user is asked to perform an initial calibration of the motors and tracking system and to set a home position to unlock the device's features. The page also allows the user to reset/deactivate the home position and recalibrate the motors and tracking system.

Activities for Wrist: allows the user to select two device modalities: automatic or manual. The automatic mode enables the typical wrist exercises, i.e. abduction/adduction, flexion/extension, and pronation/supination. Paradigmatic exercises are already available inside the GUI. For each exercise, the running time and velocity can be set both manually or directly from the interface. The manual mode enables six buttons for direct control of wrist motions.

Learning Mode Wrist: enables the exoskeleton to learn exercises performed by a physiotherapist and replay them. During the Learning mode, the device is un-tensioned, allowing the physiotherapist to freely move the user's wrist while the tracking system records the movements. IMU data are collected at 200 Hz and saved to a file via the GUI. In Reproduce mode, the user can load and replay a previously recorded exercise profile from the database.

V. Tests

The device testing is divided into two parts, *a) Device tendons system validation* and *b) Device performance*. The first focuses on comparing the results from the mathematical model in Sec. III with experimental data. The second part aims to evaluate the device's performance. The testing and evaluation phase involved a single patient, according to the "single-case-design" methodology. This approach, commonly used in the clinical field, in which an individual is the only unit of data analysis, is capable of providing robust experimental evidence [30]. The subject gave his written informed consent to participate and was able to discontinue participation at any time during the experiments. The experimental evaluation protocols followed the declaration of Helsinki, and there was no risk of harmful effects on the subject's health. Data were recorded in conformity with the European General Data Protection Regulation 2016/679, stored locally, and used only for the postprocessing evaluation procedure. No sensitive data were recorded. The subject had severe limitations in hand extension motion (movement in flexion was with reduced problems), and limitations in all the wrist movements.

a) Device tendons system validation: The user, whose anthropometric measurements were used for the simulations in Section III, was asked to wear the exoskeletal device. A specialist manually guided the user's hand to make the wrist movement profiles while the exoskeleton tracking system recorded the corresponding wrist angles. After data acquisition, the recorded profile was reproduced by the exoskeleton. The user kept his forearm on a glass support, allowing for unobstructed visualization. Two high-resolution cameras captured the motion of two markers on the tendons near the wrist. Each profile was executed four times. The recorded videos were analyzed using Kinovea software to extract marker trajectories. Two representative trials are shown in Fig. 7.

The mean ratios between wrist rotation angles and tendons' displacements were: 2.20 ± 0.11 °/mm (tendon 1) and 1.99 ± 0.12 °/mm (tendon 2) for ulnar/radial deviation, 4.88 ± 0.023 °/mm (tendon 3) for extension, 3.48 ± 0.16 °/mm (tendon 1) and 3.18 ± 0.13 °/mm (tendon 2) for flexion, and 2.10 ± 0.14 °/mm (tendon 4) and 3.32 ± 0.16 °/mm (tendon 5) for pronation/supination. It can be observed that the results are in line with the simulations, the unavoidable differences are mainly motivated by the flexibility of exoskeleton structure, which was not considered in the simulations. Moreover, to test the capability of the device to apply the required torques, a test for the evaluation of TSA module maximum force was performed. The experimental setup consisted of a vertical motorized force test rig MARK-10 F305 equipped with a FS05-200 dynamometer (accuracy 0.5 N) and a EMP001-1 distance measurement package. The hand support was removed, while the forearm support was fixed and vertically aligned with the dynamometer, which was attached to the central module of the exoskeleton. The test consisted in rotating the motor until the required torque reached 90% of its limit, keeping it for 5 s, and releasing it. The maximum force was calculated as the mean of the recorded peak forces, and resulted 121.9 ± 1.63 N (Fig. 7(c)).

b) Device performance: The tests evaluated the device performance in terms of accuracy and ability to record specific wrist exercises performed by a physiotherapist. The physiotherapist gently moved the user's hand for 10 s while the exoskeleton tracking system recorded wrist angles, representing hand orientation relative to the forearm, following three main movements i.e. adduction/abduction, flexion/extension,

IEEE Robotics and Automation Letters (RA-L) paper, presented at ICRA 2026, Vienna, Austria. Cite as RA-L paper.

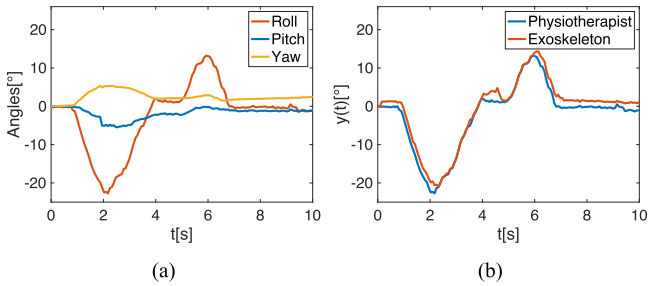

(a) (b)

Fig. 8. Pronation/supination exercise. (a) Roll, pitch, yaw angles measured by the tracking system during manual exercises with a therapist. (b) representative playback trial with the exoskeleton.

and pronation/supination. By using the exoskeleton, ten consecutive repetitions were conducted for each profile, and wrist angle data were tracked for each repetition. A representative trial for pronation/supination is shown in Fig. 8. The figure shows the capability of the wrist exoskeleton to record wrist movement with respect to the forearm and to playback the motion by exploiting the tracking system.

For all experiments, the Root Mean Square Error (RMSE) was considered as a metric to define the device precision in following a desired profile. Similarly to [31], for each trial we define this quantity as $RMSE_t = \sqrt{\frac{1}{N}\sum_{i=1}^{N}(y_{t,i} - y_i)^2}$, where N is the number of samples in a trial, y_i is the actual value, and $y_{t,i}$ is the corresponding target value. Moreover, it was used the mean among the RMSE to have insights of the tracking performance throughout the whole experiment. It is worth noticing that the tracking RMSE is an effective metric for assessing both the speed and accuracy of the robot's movements. This is because the RMSE increases when the exoskeleton is either slow in updating the control variable or fails to reach the target value. The average RMS errors in performing the profile previously recorded by the physiotherapist were $0.92° \pm 0.15°$ for flexion/extension, $1.00° \pm 0.15°$ for abduction/adduction and $0.95° \pm 0.15°$ for pronation/supination.

Qualitative Assessment: After the experimental evaluation, the user assessed the system by reporting his impressions and comments. Four aspects were considered: Ergonomics and safety, Wearability, Ease of Control, and Portability. User's feedback and experiment results allowed to draw an overall evaluation of the system with respect to the existing solutions.

VI. Discussion

In this section, we frame the main characteristics of the proposed device, following the roadmap for the design and classification of wearable devices in [32].

Actuation: The proposed device can actuate flexion/extension, ulnar/radial deviation, and prono/supination movements of the wrist, the system is therefore 3-DoFs. Compared to previously proposed devices, described in [4], [33], the system is improved with the possibility of actuating the pronation/supination movement. Due to the compact design of the device, the tendons which provide wrist abduction/adduction may cause undesired flexion movements, but the undesired motion can be mitigated by increasing the tension of the extension tendon.

Range of motion: Wrist kinematics and joint ROM have been analyzed in the preliminary phase of the design. In this study we considered the ROM values proposed in [27] and summarized in Table I. The actuation system, based on 5 tendons, allows bidirectional movements. The system can switch between tensioned tendons status and untensioned tendons status thanks to the different control methods. Untensioned tendons are needed in the recording phase, when the exercise is supported by the therapist while the movement is acquired by the tracking system.

Ergonomics and safety: The device is designed for user comfort during extended use, and is lighter and more compact compared to other solutions (e.g. [4], [33]). Weighing 246 g (excluding batteries and electronics), it is comparable to similar designs, such as the 300 g device in [33]. User safety is prioritized in both hardware and software. The system can be deactivated at any time via a button on the electronic box or from the GUI 'Stop' button. In the event of motor failures that could block the exoskeleton, the interrupted anchor points, the tunnels, and the motors are easily removable.

Wearability: The exoskeleton design is adaptable, allowing users to customize it based on their requirements and anthropometric measurements for a personalized experience. Its lightweight and flexible construction, combined with TSA-based actuation, minimizes user fatigue, enabling extended periods of usage without experiencing pain.

Control: Similarly to previously developed devices, the solution presented in this letter implements a position control, with the possibility of executing pre-defined or pre-recorded exercises. A position control strategy has been chosen, rather than impedance or admittance one, to make the system simpler and accessible to the user.

Portability: The device is compact and light for autonomous and comfortable use. Batteries, actuators, and transmission systems allow a completely wireless system. The device has been developed to be fully capable of being operated autonomously by the patient at home.

VII. Conclusion

This letter presents the design and development of a TSA-based wrist exoskeleton for rehabilitation and training. The device enables controlled wrist movements with high force output and low energy consumption, making it suitable for extended rehabilitation sessions. It supports wrist exercises, which can either be recorded in collaboration with a physiotherapist through the *Learning Mode Wrist* GUI page or selected from the predefined exercise available in the *Activities for Wrist* page. Preliminary experiments confirm its ability to replicate natural wrist movements, highlighting its potential for personalized rehabilitation. Future work will focus on refining the analytical models and control algorithms for more complex wrist movements (e.g. wrist rotation/circumduction), integrating real-time sensing mechanisms, incorporating artificial intelligence for intention-based patient control, and conducting clinical trials to validate therapeutic effectiveness. The ultimate goal is to create an affordable, portable, and effective wrist rehabilitation tool bridging the gap between clinical and at-home recovery.

Acknowledgment

The author sincerely thank Alessio Piroli for his thoughtful insights and dedicated support during the testing phase, which played a key role in shaping the outcomes of this work.

IEEE Robotics and Automation Letters (RA-L) paper, presented at ICRA 2026, Vienna, Austria. Cite as RA-L paper.

REFERENCES

[1] S. Hussain, P. K. Jamwal, P. Van Vliet, and M. H. Ghayesh, "State-of-the-art robotic devices for wrist rehabilitation: Design and control aspects," *IEEE Trans. Hum.- Mach. Syst.*, vol. 50, no. 5, pp. 361–372, Oct. 2020.

[2] R. F. Pitzalis, D. Park, D. G. Caldwell, G. Berselli, and J. Ortiz, "State of the art in wearable wrist exoskeletons part I: Background needs and design requirements," *Machines*, vol. 11, no. 4, 2023, Art. no. 458.

[3] R. F. Pitzalis, D. Park, D. G. Caldwell, G. Berselli, and J. Ortiz, "State of the art in wearable wrist exoskeletons part II: A review of commercial and research devices," *Machines*, vol. 12, no. 1, p. 21, 2024.

[4] M. Dragusanu, M. Z. Iqbal, T. Lisini Baldi, D. Prattichizzo, and M. Malvezzi, "Design, development, and control of a hand/wrist exoskeleton for rehabilitation and training," *IEEE Trans. Robot.*, vol. 38, no. 3, pp. 1472–1488, Jun. 2022.

[5] M. Tiboni, A. Borboni, F. Vérité, C. Bregoli, and C. Amici, "Sensors and actuation technologies in exoskeletons: A review," *Sensors*, vol. 22, no. 3, 2022, Art. no. 884.

[6] M. Dragusanu, D. Troisi, B. Suthar, I. Hussain, D. Prattichizzo, and M. Malvezzi, "MGlove-ts: A modular soft glove based on twisted string actuators and flexible structures," *Mechatronics*, vol. 98, 2024, Art. no. 103141.

[7] J. Zhang et al., "Robotic artificial muscles: Current progress and future perspectives," *IEEE Trans. Robot.*, vol. 35, no. 3, pp. 761–781, Jun. 2019.

[8] M. A. Khan, B. Suthar, I. Gaponov, and J.-H. Ryu, "Single-motor-based bidirectional twisted string actuation with variable radius pulleys," *IEEE Robot. Automat. Lett.*, vol. 4, no. 4, pp. 3735–3741, Oct. 2019.

[9] G. Palli, C. Natale, C. May, C. Melchiorri, and T. Wurtz, "Modeling and control of the twisted string actuation system," *IEEE/ASME Trans. Mechatron.*, vol. 18, no. 2, pp. 664–673, Feb. 2013.

[10] I. Gaponov, D. Popov, and J.-H. Ryu, "Twisted string actuation systems: A study of the mathematical model and a comparison of twisted strings," *IEEE/ASME Trans. Mechatron.*, vol. 19, no. 4, pp. 1331–1342, Apr. 2014.

[11] G. Palli et al., "The DEXMART hand: Mechatronic design and experimental evaluation of synergy-based control for human-like grasping," *Int. J. Robot. Res.*, vol. 33, no. 5, pp. 799–824, 2014.

[12] I. Gaponov, D. Popov, S. J. Lee, and J.-H. Ryu, "Auxilio: A portable cable-driven exosuit for upper extremity assistance," *Int. J. Control, Automat. Syst.*, vol. 15, no. 1, pp. 73–84, 2017.

[13] M. Hosseini, A. Sengül, Y. Pane, J. De Schutter, and H. Bruyninck, "ExoTen-Glove: A force-feedback haptic glove based on twisted string actuation system," in *Proc. 27th IEEE Int. Symp. Robot Hum. Interactive Commun.* (RO-MAN), 2018, pp. 320–327.

[14] T. Tsabedze, E. Hartman, E. Abrego, C. Brennan, and J. Zhang, "TSA-BRAG: A twisted string actuator-powered biomimetic robotic assistive glove," in *Proc. 2020 Int. Symp. Med. Robot. (ISMR)*, 2020, pp. 159–165.

[15] M. Hosseini, R. Meattini, G. Palli, and C. Melchiorri et al., "A wearable robotic device based on twisted string actuation for rehabilitation and assistive applications," *J. Robot.*, vol. 2017, 2017.

[16] T. Tsabedze, E. Hartman, C. Brennan, and J. Zhang, "A compliant robotic wrist orthosis driven by twisted string actuators," in *Proc. 2021 Int. Symp. Med. Robot. (ISMR)*, 2021, pp. 1–7.

[17] C. Greco, T. H. Weerakkody, V. Cichella, L. Pagnotta, and C. Lamuta, "Lightweight bioinspired exoskeleton for wrist rehabilitation powered by twisted and coiled artificial muscles," *Robotics*, vol. 12, no. 1, 2023, Art. no. 27.

[18] P. Muehlbauer, M. Schimbera, K. Stewart, and P. P. Pott, "Twisted string actuation for an active modular hand orthosis," in *Proc. ACTUATOR; Int. Conf. Exhib. New Actuator Syst. Appl. 2021*, VDE, 2021, pp. 1–4.

[19] M. Dragusanu, D. Troisi, B. Suthar, D. Prattichizzo, and M. Malvezzi, "Development of a soft actuated glove based on twisted string actuators for hand rehabilitation," in *Proc. 10th IEEE RAS/EMBS Int. Conf. Biomed. Robot. Biomechatronics* (BioRob),, 2024, pp. 1702–1708.

[20] J. Wang, W. Zhang, T. Guo, and Y. Zhou, "Smart flexible wrist exoskeleton with twisted string actuators and IMU feedback," in *Proc. 2024 7th Int. Conf. Robot., Control Autom. Eng. (RCAE)*, 2024, pp. 22–26.

[21] C. E. Lang et al., "Observation of amounts of movement practice provided during stroke rehabilitation," *Arch. Phys. Med. Rehabil.*, vol. 90, no. 10, pp. 1692–1698, 2009.

[22] M. Malvezzi, G. Gioioso, G. Salvietti, and D. Prattichizzo, "SynGrasp: A MATLAB toolbox for underactuated and compliant hands," *IEEE Robot. Automat. Mag.*, vol. 22, no. 4, pp. 52–68, Dec. 2015.

[23] E. Peña-Pitarch, N. T. Falguera, and J. Yang, "Virtual human hand: Model and kinematics," *Comput. Methods Biomech. Biomed. Eng.*, vol. 17, no. 5, pp. 568–579, 2014.

[24] I. M. Bullock, J. Borràs, and A. M. Dollar, "Assessing assumptions in kinematic hand models: A review," in *Proc. 4th IEEE RAS EMBS Int. Conf. Biomed. Robot. Biomechatronics* (BioRob), 2012, pp. 139–146.

[25] M. Rainbow, A. Wolff, J. Crisco, and S. Wolfe, "Functional kinematics of the wrist," *J. Hand Surg. (Euro. Vol.)*, vol. 41, no. 1, pp. 7–21, 2016.

[26] K. Park, P.-H. Chang, and S. H. Kang, "*In vivo* estimation of human forearm and wrist dynamic properties," *IEEE Trans. Neural Syst. Rehabil. Eng.*, vol. 25, no. 5, pp. 436–446, May 2017.

[27] J. C. Perry, J. Rosen, and S. Burns, "Upper-limb powered exoskeleton design," *IEEE/ASME Trans. Mechatron.*, vol. 12, no. 4, pp. 408–417, Apr. 2007.

[28] K.-Y. Wu, Y.-Y. Su, Y.-L. Yu, C.-H. Lin, and C.-C. Lan, "A 5-degrees-of-freedom lightweight elbow-wrist exoskeleton for forearm fine-motion rehabilitation," *IEEE/ASME Trans. Mechatron.*, vol. 24, no. 6, pp. 2684–2695, Dec. 2019.

[29] T. Würtz, C. May, B. Holz, C. Natale, G. Palli, and C. Melchiorri, "The twisted string actuation system: Modeling and control," in *Proc. IEEE/ASME Int. Conf. Adv. Intell. Mechatron.*, 2010, pp. 1215–1220.

[30] T. R. Kratochwill et al., "Single-case designs technical documentation," *What Works Clearinghouse*, Inst. Educ. Sci., U.S. Dept. Educ., 2010.

[31] D. Ao, R. Song, and J. Gao, "Movement performance of human–robot cooperation control based on emg-driven hill-type and proportional models for an ankle power-assist exoskeleton robot," *IEEE Trans. Neural Syst. Rehabil. Eng.*, vol. 25, no. 8, pp. 1125–1134, Aug. 2017.

[32] G. M. Achilli et al., "Soft, rigid, and hybrid robotic exoskeletons for hand rehabilitation: Roadmap with impairment-oriented rationale for devices design and selection," *Appl. Sci.*, vol. 13, no. 20, 2023, Art. no. 11287.

[33] M. Dragusanu, T. Lisini Baldi, Z. Iqbal, D. Prattichizzo, and M. Malvezzi, "Design, development, and control of a tendon-actuated exoskeleton for wrist rehabilitation and training," in *Proc. IEEE Int. Conf. Robot. Automat. (ICRA)*, 2020, pp. 1749–1754.